

**AN EMPIRICALLY BASED MODEL FOR PREDICTING
INFRARED LUMINOSITY FUNCTIONS, DEEP INFRARED
GALAXY COUNTS AND THE DIFFUSE INFRARED
BACKGROUND**

M. A. Malkan

Physics and Astronomy Department, University of California Los Angeles, Los Angeles, CA

90095-1562

malkan@astro.ucla.edu

F. W. Stecker

Laboratory for High Energy Astrophysics, NASA Goddard Space Flight Center, Greenbelt,

MD 20771

stecker@lheapop.gsfc.nasa.gov

Received _____; accepted _____

ABSTRACT

We predict luminosity functions and number counts for extragalactic infrared sources at various wavelengths using our empirically based model. This is the same model which we used successfully to previously predict the spectral energy distribution of the diffuse infrared background. Comparisons of galaxy count results with existing data indicate that either galaxy luminosity evolution is not much stronger than $Q = 3.1$ (where $L \propto (1+z)^Q$) or this evolution does not continue to strengthen beyond a redshift of 2. However, measurements of the far infrared background from *COBE-DIRBE* (Cosmic Background Explorer–Diffuse Infrared Background Experiment) seem to suggest a stronger evolution for the far-infrared emission, with $Q > 4$ in the redshift range between 0 and 1. We discuss several interpretations of these results, and also discuss how future observations can reconcile this apparent conflict. We also make predictions of the redshift distributions of extragalactic infrared sources at selected flux levels which can be tested by planned detectors. Finally we predict the fluxes at which various future surveys will become confusion limited.

Subject headings: infrared sources, galaxies, background radiations

1. Introduction: Motivation for Extending Previous Work

Observational cosmology is just starting to benefit from unprecedented sensitivity gains at wavelengths longward of $1 \mu\text{m}$. A prime example is the breakthrough achieved by the COBE satellite in the first detections of the Diffuse Infrared Background (DIRB) radiation at wavelengths from 2 to $300 \mu\text{m}$. These measurements provide crucial information about the integrated luminosity of galaxies. Especially at the longer wavelengths, where the K-corrections of individual galaxies actually become positive, the DIRB measurements actually constrain the evolution of the galactic luminosity function (LF) back to cosmologically interesting redshifts ($z \geq 0.5$).

To elucidate these constraints, we started with the simple empirically based model which we used previously to calculate the DIRB (Malkan and Stecker 1998, MS98 hereafter). In MS98, we made use of infrared observations of galaxies over a wide range of luminosities and at various wavelengths. We assumed that the systematic dependence of galaxy spectra with luminosity which we observe today also applies at earlier cosmic times. We then started with the present-day infrared luminosity function of galaxies, and assumed a pure luminosity evolution for each galaxy, with $L \propto (1+z)^{3.1}$ out to a redshift of z_{flat} of 1 or 2, beyond which no further evolution occurred. This “backwards evolution” model gave predictions of the DIRB which were generally confirmed by subsequent *COBE* data.

Encouraged by the accuracy of the DIRB predictions obtained from our empirically based model (MS98), we use it in this paper to derive luminosity functions at various infrared wavelengths and to make infrared galaxy count predictions. These calculations should provide timely predictions which will aid in the planning and interpretation of ongoing and new deep infrared imaging observations and their implications in understanding galaxy formation and evolution.

Several new telescopes have, or soon will obtain deep extragalactic number counts of infrared and millimeter sources in large regions of the sky at high galactic latitude which are rela-

tively free of galactic foreground infrared emission. Surveys have recently been completed with the *ISOCAM* Infrared Space Observatory Camera) and *ISOPHOT* (Infrared Space Observatory Photometer) imagers on the Infrared Space Observatory, *ISO* and with *SCUBA* (Submillimeter Common User Bolometer Array) on the James Clerk Maxwell Telescope. Several new ones are planned, *e.g.*, with *SIRTF* (Space Infrared Telescope Facility), *SOFIA* (Stratospheric Observatory for Infrared Astronomy), *IRIS* (Infrared Imaging Surveyor), and *FIRST* (Far Infrared and Submillimeter Telescope).

Even though spectroscopic redshifts are difficult to obtain for more than a handful of the faint infrared sources, there is a high likelihood that a significant fraction of them is at cosmologically interesting distances. Thus, deep galaxy number counts of sufficiently large areas will provide statistical information about galaxies at large lookback times, and therefore about galaxy formation and evolution. We use our model here to predict such number counts. We also re-examine our predictions of the spectral energy distribution (SED) of the DIRB, in light of the subsequent *COBE* results.

If redshifts can also be measured (spectroscopically or photometrically) for statistically significant subsamples of faint infrared sources, even more details of the evolution can be determined. Therefore, in this paper we also make predictions of the redshift distributions of galaxies at selected flux levels which will be accessible in the future. Finally, we use the model predictions to estimate the flux levels at which various surveys should become confusion limited.

2. Galaxy Spectral Energy Distributions

The two key factors determining the infrared counts are the evolution of star formation rates, and the amount and distribution of dust grains in galaxies as a function of luminosity and time. Growing observational evidence indicates that the dust contents of high-redshift

galaxies was not very different from what is observed in present day galaxies (see Malkan 1998; 2000 for reviews). The more luminous low-redshift galaxies contain enough dust around their actively star-forming complexes to absorb much of the ultraviolet continuum light, and re-emit it in the mid infrared and far infrared. The ratio of infrared luminosity to blue and ultraviolet luminosity can exceed one, and this ratio is observed to be a *systematically increasing function of galaxy luminosity*, or current star formation rate (Spinoglio *et al.* 1995). Furthermore, the enhanced dust emission in luminous galaxies arises from relatively warm grains which emit at 25 to 60 μm . We have made the simplifying assumption that the same systematic correlations of dust content and resulting spectral shape as a function of luminosity that we measure at $z \sim 0$ also apply to galaxies at large redshift.

MS98 used the correlations of bolometric luminosity with the luminosities at 12, 25, 60 and 100 μm from Spinoglio *et al.* (1995) to define the spectral shape of galaxies as a function of their luminosities at L_{60} or L_{12} , their luminosities at 60 μm and 12 μm respectively. In the near infrared, constant spectral shapes were assumed with intrinsic zero-redshift average colors of $J - H = [1.2\mu\text{m} - 1.6\mu\text{m}] = 0.9$ mag and $H - K = [1.6\mu\text{m} - 2.2\mu\text{m}] = 0.4$ mag.

At long wavelengths, MS98 assumed greybody thermal emission appropriate for dust grains with emissivity $\propto \lambda^{-1.5}$, following the correlation in Appendix B of Spingolio *et al.* (1995). In this paper we have improved the description of the emission longward of 100 μm , the last *IRAS* (Infrared Astronomy Satellite) band. We have used the growing sets of 60 to 200 μm galaxy photometry data becoming available from the *ISOPHOT* instrument on *ISO*. As summarized by Spinoglio *et al.* (2000), new far-infrared photometry is now available for dozens of nearby galaxies which span a wide range in luminosity. These observations confirm the prediction of Spinoglio *et al.* (1995) that the galaxies with “warmer” (i.e. bluer or flatter) 60 to 100 μm spectral slopes also appear warmer in the 100 to 200 μm region, where their thermal dust spectra approach a Rayleigh-Jeans distribution modified by dust emissivity $\propto \lambda^{-n}$ where $1.5 \leq n \leq 2$. We also confirm their finding that the warmer dust (associated with regions of recent star

formation) increases the 60 μm flux relative to the flux longward of 100 μm systematically in the more infrared-luminous galaxies.

Thus we are able to use these *ISOPHOT* observations to make a direct calibration of the average long-wavelength spectrum of galaxies as a function of their 60 μm luminosity. We describe the 100–200 μm spectra as a broken power law with a break at 145 μm . The slopes above and below 145 μm have the same luminosity dependence

$$\alpha_{100-145} = -0.65 + 0.6 \log(L/L_*) \quad (1a)$$

and

$$\alpha_{145-200} = +2.0 + 0.6 \log(L/L_*) \quad (1b)$$

where L_* is the luminosity of a typical normal galaxy at 60 μm , 10^{43} erg s^{-1} .

3. Galaxy Luminosity Functions

In our calculation, the four luminosity relations obtained by Spinoglio *et al.* (1995) at 12, 25, 60 and 100 μm (and our estimates at 2.2 and 3.5 μm) were inverted so that a luminosity at any given rest wavelength could be determined from the 60 μm luminosity, L_{60} . This allowed us to make a mapping of the 60 μm luminosity function (LF) of Lawrence *et al.* (1986) into LFs at any infrared wavelength using the transformation relation

$$\phi_\lambda(\log L_\lambda) = \phi_{60}(\log L_{60})(d \log L_{60} / d \log L_\lambda) \quad (2)$$

Given the fairly good scaling of other wavelengths with the 60 μm luminosity, the Jacobian term on the right (which conserves total number of galaxies) varies from 1.0 in the 25 to 60 μm range, up to 1.25 at 12 and 300 μm .

MS98 made calculations with 60 μm LFs from Saunders *et al.* (1990) and from Lawrence *et al.* (1986). In this paper we adopt the parameters from Lawrence *et al.* (1986), *viz.*, $\alpha = 1.7$

and $\beta = 1.8$ with a normalization constant of $C = 4.07 \times 10^{-4}$, because they give a better match to the local 60 μm counts. In Figure 1 we show the galaxy luminosity functions at a redshift of 0 based on our model.

The 12 μm LF has essentially the identical shape to the *bolometric* LF of non-Seyfert galaxies, because the 12 μm flux is a constant 6% of the bolometric flux for all galaxy types except normal ellipticals (Spinoglio *et al.* 1995). By comparison, the 25 μm and 60 μm LFs are flatter. They extend out more strongly to high luminosities because high-L galaxies emit a relatively larger fraction of their bolometric luminosities at 25 to 60 μm . Conversely, the 3 μm and 400 μm LFs are much steeper. This is because it is the less luminous galaxies which emit relatively more power at 3 μm and 400 μm .

For comparison, we also plot estimated local luminosity functions at 12, 25, 60 and 100 μm , taken from the literature. The particular fiducial LF we have used was specifically fitted to the 60 μm data points (shown as solid squares). Thus it is not surprising that the model LF (solid line) matches these observations extremely well. The validity of our wavelength transformation equations is confirmed by comparison of our model LF's with data at longer and shorter wavelengths. The 25 μm and 100 μm data (X's and open squares, respectively) are both from Soiffer *et al.* (1991). Our model LF has a slightly flatter slope than these data, but with essentially identical overall normalizations. Our model LF at 12 μm (dot-dash line) agrees well with the data from Rush, Malkan & Spinoglio (1993—solid circles, which include AGN in the totals). New determinations of the 12 μm and 15 μm LF's (open triangles from Xu *et al.* 1998) find substantially fewer low luminosity galaxies. The reason for this is well understood: in contrast to the other LF estimates, these two new determinations were corrected for the overdensity of nearby low luminosity galaxies in the Virgo cluster. These two corrected LFs are thus believed to be more representative of the present day Universe. However, if we are using LF's to predict number counts of bright sources in the Northern sky, the actual local LF of Rush *et al.* (1993) would give more accurate results. In any case, our use of the Lawrence

et al. (1986) LF is an excellent compromise fit to all of the local *IRAS* data from 12 to 100 μm .

Fortunately, none of these subtleties makes any significant difference in the predicted counts. This is because the characteristic bent shape of the LF guarantees that the counts at any flux level are always dominated by the number of galaxies around the characteristic position of the knee in the LF, defined to be L_* . As long as all the LF's are accurate around L_* (where there is virtually no disagreement), they will yield almost exactly the correct source number counts.

Since MS98 demonstrated that active galaxies (AGN) contribute less than 10% of the diffuse extragalactic infrared background, a fraction within the errors of the models and the data, we neglect the AGN component to the DIRB in this work.

4. Galaxy Evolution

The luminosity functions at higher redshifts were calculated using the pure evolution relations

$$\phi[L_\nu, \lambda; z] = \phi_{MS, z=0}[L_{\nu/(1+z)}/(l+z)^Q, (1+z)\lambda] \quad (3)$$

where

$$\phi_{MS, z=0} = [C(L/L_*)^{1-\alpha}[1 + (L/\beta L_*)]^{-\beta}]_{60} d \log \phi_{60} / d \log \phi(\lambda) \quad (4)$$

where the subscript 60 refers to a wavelength of 60 μm and P and Q are the galaxy number and luminosity evolution parameters, respectively. We note that these are differential luminosity functions and that we follow the common convention where they are measured per unit logarithmic interval of luminosity.

We adopted the same evolutionary assumption as MS98, pure luminosity evolution with all galaxy luminosities scaling as $(1+z)^{3.1}$ (*i.e.*, $P = 0, Q = 3.1$) up to a redshift $z_{flat} = 2$ with

a cutoff at $z_{max} = 4$. For example, the LF curves for $z = 1$ are identical to the corresponding ones at $z = 0$ for wavelengths twice as long, with a suitable scaling of $2^{3.1}$ in the (horizontal) luminosity axis.

The “Best Estimate” galaxy evolution model used by MS98 to predict the diffuse infrared background took $Q = 3.1$ and $z_{flat} = 2$.¹ Here we refer to this model as the “Baseline” model.

As observations of high-redshift galaxies improved, they have tended to reinforce our earlier redshift evolution assumptions as providing a realistic description of the cosmic evolution of galaxy luminosities (Madau, Pozzetti & Dickinson 1998, Steidel, *et al.* 1999, Blain & Natarajan 2000; Hopkins, Connolly & Szalay 2000).

MS98 also showed a more conservative calculation, in which the luminosity evolution (with Q still equal to 3.1) was frozen at $z_{flat} = 1$. Thus by $z = 2$, this conservative scenario assumes galaxy luminosities were only $2^{3.1}$ times more luminous than today, rather than the factor of $3^{3.1}$ assumed in the baseline model. In this paper, we refer to the $z_{flat} = 1$; $Q = 3.1$ model as the “Lower Limit” scenario.

We also consider here an alternate “Fast Evolution” scenario, in which the evolution index is increased to $Q = 4.1$, while z_{max} is taken to be 1.3. As for the baseline case, this scenario also implies that galaxies were forming stars at ~ 30 times higher rates at $z = 2$ than today. However, with fast evolution, the galaxy luminosities at $z = 1.3$ were also ~ 30 times higher, in contrast to the baseline model in which they were 8.6 times their current luminosities. Support for the Fast Evolution scenario is found in the recent *NICMOS* (Near Infrared Camera and Multi-Object Spectrograph) studies of Hopkins *et al.* (2000).

¹In generating Figure 2 of MS98, galaxies above $z = 2$ were erroneously assumed to have the same luminosities as at $z = 0$. Here we more properly assume that the LF has evolution up to z_{flat} and no further evolution beyond that. Our corrected result and that given in MS98 are not significantly different.

5. Diffuse Infrared Background Radiation

First we compare the predictions of our model with the new measurements of the DIRB as shown in Figure 2. The baseline model with $Q = 3.1$, $z_{max} = 4$ and $z_{flat} = 2$, is shown by the middle solid line. The lower dashed curve is the prediction of our lower limit model with $z_{flat} = 1$. The upper (dot-dashed) curve shows our fast evolution ($Q = 4$; $z_{flat} = 1.3$) case.

The predicted DIRB is most sensitive to the exponent of the luminosity evolution, Q . Increasing or decreasing Q by 0.5 results in a DIRB which increases or decreases by 25 to 30% at most wavelengths. The second most important parameter is the redshift at which the luminosity evolution stops, which was $z_{flat} = 2$ in the baseline calculation. If z_{flat} is dropped to 1 with Q unchanged, the DIRB drops by about 25% at most wavelengths, as is evident from the lower dashed curve. Finally, the least important free parameter is the maximum redshift for which infrared emitting galaxies are included, $z_{max} = 4$ in the baseline case. When this z_{max} is decreased to 2, the DIRB decreases by about 30% at most wavelengths. The combination of redshift evolution and cosmology insures that it is the galaxies at redshifts ~ 1 which contribute most to the DIRB, as discussed further below.

In our lower limit case, the redshift of maximum evolution is reduced to $z_{flat} = 1$ while Q is taken to be to 3.1, resulting in a DIRB prediction about 15 to 20% lower than our baseline case. Our fast evolution case gives DIRB fluxes which are about 80% higher than our baseline case at mid infrared and far infrared wavelengths. All of our models are consistent with the subsequent *COBE* detections of the cosmic background at 2.2 μm and 3.5 μm (Dwek and Arendt 1998; Gorjian, Wright & Chary 2000). However, our fast evolution case appears to be more consistent with the *COBE* determinations at 140 and 240 μm (Hauser, *et al.* 1998) to within 2 standard deviations (neglecting systematic errors).

We note that the best constraint on the DIRB at mid-infrared wavelengths comes from studies of the lack of absorption features in blazar spectra up to 10 TeV. This gives an upper

limit on the $20\,\mu\text{m}$ flux of 4 to $5\,\text{nW m}^{-2}\text{sr}^{-1}$ (Stecker & de Jager 1997, Stanev & Franceschini 1998; Biller *et al.* 1998). This limit, when combined with our predicted DIRB SEDs, disfavors evolution with $Q > 5$.

6. Observational Appearance of a Typical Evolving Galaxy

The redshift distribution can be understood by considering the brightness of a typical bright galaxy, viewed out to various redshifts. For example, let us consider a galaxy with a current $60\,\mu\text{m}$ luminosity of L_* at the knee in the LF. The observed flux of a galaxy whose present luminosity is L_* , given as a function of redshift, is shown in Figure 3 for observing wavelengths of 25, 60 and $200\,\mu\text{m}$. Observing an L_* galaxy at a fixed wavelength samples emission at progressively shorter rest-system wavelengths at progressively higher redshifts. For a wavelength of $200\,\mu\text{m}$, the peak of the far infrared spectrum of this galaxy is shifted into the observing bandpass at $z \sim 1$, resulting in a negative K-correction. This explains the relatively flat portion of the flux curve from $z = 0.6$ to 1.0. At higher redshifts, luminosity evolution produces an even stronger effect, which causes all the flux curves to become relatively flat from $z = 1.5$ to 2.0.

Figure 3 also shows the $60\,\mu\text{m}$ fluxes of galaxies which are currently 100 times more or less luminous than L_* are shown by the dotted and dashed lines. At an observing wavelength of $60\,\mu\text{m}$, evolutionary changes in galaxy spectra make the less luminous galaxies relatively brighter at high redshifts.

7. Galaxy Number Counts

We can sum our generated family of LFs over redshift to obtain the expected number of observable sources at a given flux level and wavelength over the entire sky:

$$dN/dF(\lambda_0) = 16\pi(c/H_0)^3 \int_0^{z_{max}} dz \int_{L_{min}(F,z)}^{\infty} (d\log L)\phi(\lambda_0/(1+z), z)(1+z)^{-5/2}(\sqrt{(1+z)-1})^2 \quad (5)$$

assuming $\Omega = 1$ and $\Lambda = 0$. Figure 4 shows the predicted integrated galaxy counts as a function of minimum observable flux at each of the 8 logarithmically spaced wavelengths shown in Figure 1.

As expected, the slopes of the integrated counts are approximately equal to the Euclidean value (-3/2) at the brighter flux levels (above 1 mJy). The galaxy counts from 2 μ m to 100 μ m have similar slopes with a Euclidean (high-flux) normalization (in Jansky flux units) given by the formula:

$$\text{Log}F^{3/2}N(> F) = 0.46 - 0.06\text{Log}(\lambda) + 0.83(\text{Log}\lambda)^2 \quad (6)$$

reflecting the average spectral spectral energy distribution of a typical L_* galaxy. However, the characteristic knee where the slope flattens is shifted to higher flux levels at longer wavelengths. This reflects the fact that an L_* galaxy is more luminous at longer wavelengths, and can therefore be seen to larger distances. The 3 and 6 μ m counts rise above the Euclidean value briefly around 0.1 mJy, owing to the positive K-corrections at those wavelengths. At fluxes fainter than 0.1 mJy, the counts at all wavelengths are flatter than the Euclidean slope, because the deviations due to cosmology dominate over galaxy evolution, which was assumed to level off at $z > 2$. At 50 and 100 μ m, this cosmological flattening of the counts slope occurs at 1 to 10 mJy, the brightness of typical L_* galaxies at redshifts greater than 1. At longer wavelengths, between 200 and 400 μ m, on the falling side of the peak of the rest-frame energy distribution, there is hardly any flux range where the counts slope is Euclidean. The counts at the *bright* end, from 1 to 0.01 Jy, actually rise more steeply than the -1.5 slope, owing to the strong K-corrections for redshifts up to ~ 1 to 2. For long-wavelength fluxes below 0.01 Jy, the counts curves flatten from the contributions of galaxies at redshifts of 2 and higher.

Our predicted counts at all wavelengths have a steeper slope (more faint sources) than those of Takeuchi *et al.* (1999), because our assumed evolution ($Q = 3.1$) is twice as much as

theirs ($Q = 1.4$ or 1.5). Our predicted 15 , 60 and $175\,\mu\text{m}$ counts are closer to those of Tan *et al.* (1999), although 10 to 40% higher, because our assumed $Q = 3.1$ evolution is effectively stronger up to $z = 2$ than that of their disk galaxies (which dominate much of the counts at these wavelengths). Our counts slopes are steeper than those of model E of Guiderdoni *et al.* (1998). We predict two to three times more faint sources at $15\mu\text{m}$, 50% more at $60\mu\text{m}$, and only slightly more faint sources at $175\mu\text{m}$. The *shape* of our number count curves agrees very well with those of Xu *et al.* (1998), as it must, because we both used virtually identical methodology and luminosity evolution assumptions. However, the *normalization* of our counts is higher by about a factor of two (more at $15\mu\text{m}$, and less at $25\mu\text{m}$), because of the differences in our assumed local LF's.

In Figures 5 and 6 we compare the predictions of our three models with observations of faint integral source counts at $15\mu\text{m}$ and $175\mu\text{m}$, respectively. The $15\mu\text{m}$ source count data are taken from the recent compilations by Serjeant *et al.* (2000) for the brighter fluxes (shown by the thick line), and Elbaz *et al.* (2000) for the fainter fluxes and are mostly based on various deep *ISOCAM* fields. The $175\mu\text{m}$ counts are taken from a compilation by Dole *et al.* (2000) and Juvela *et al.* (2000), based on deep *ISOPHOT* imaging in the *FIRBACK* (Far Infrared Background) survey. The three model predictions are again shown as a solid line for the baseline case, a dashed line for the fast evolution case, and a dot-dashed line for the lower limit case. Our new description of the long-wavelength spectrum increased the predicted number counts at $175\,\mu\text{m}$ by about 30% over our pre-*ISOPHOT* estimate. This change, of course, does not effect the counts at shorter wavelengths.

The observed faint counts at both mid- and far infrared wavelengths agrees with our baseline model. The only apparent discrepancy occurs around intermediate $15\mu\text{m}$ fluxes, where the counts from the Marano fields fall significantly below comparable measurements from other data sets. It appears, in fact, that much of this apparent disagreement is attributable to different choices of flux calibration by the different *ISOCAM* teams (Elbaz *et al.* 2000). The

predictions of the “Lower Limit” model with truncated evolution at $z_{flat} = 1$ is so similar to the baseline model that they are also close to the observations. With $Q = 3.1$, changing z_{flat} from 2 to 1 decreases the predicted number of 0.1 mJy sources at $15\mu\text{m}$ by only 20%. With $z_{flat} = 1$, increasing Q from 3.1 to 4.1 results in a 30% increase in bright (1 Jy) $175\mu\text{m}$ sources. However, extending evolution with $Q = 4.1$ up to $z_{flat} = 1.3$ leads to a prediction of 40 to 50% more faint sources, in apparent conflict with most of the observations. Certainly a very fast evolution case ($Q = 5$) is ruled out, as it significantly overpredicts (by 75% or more) the number of 15 and $175\mu\text{m}$ sources.

8. Predicted Redshift Distributions for Future Surveys

The range of plausible models calculated above all predict DIRB spectra and galaxy number counts at wavelengths from 3 to $400\mu\text{m}$ which differ by at most a factor of 2.5. These models also differ in their predictions of the redshift distributions of faint galaxies. We now show how even limited redshift information for flux-limited galaxy samples will discriminate between these models.

Several planned deep imaging surveys of low-foreground regions of the sky should be sensitive enough to detect a significant fraction of the galaxy population at moderate and very high redshifts. In early 2003, the *SIRTF* “First Look Survey” should detect galaxies with fluxes of 1 mJy at $25\mu\text{m}$ and 5 mJy at $70\mu\text{m}$ with the Multiband Imaging Photometer, *MIPS*. *SIRTF* First Look Survey imaging with the Infrared Array Camera, *IRAC* will detect $30\mu\text{Jy}$ sources at $6\mu\text{m}$. In the same year, a wider sky area will be surveyed at $120\mu\text{m}$ by *IRIS* (Shibai, 2000).

In Figure 7 we assume that it will detect galaxies down to 32 mJy. Several years later, surveys with the Photoconductor Array Camera and Spectrometer, *PACS* on the Far Infrared Space Telescope, *FIRST* will detect 1 mJy sources at $200\mu\text{m}$.

The integrand of Eq. (4) evaluated at a fixed observing wavelength down to a given flux

limit gives the differential redshift distribution, dN/dz . We plot this distribution in Figures 7a and 7b for sample deep observations at 6, 25, 120 and 200 μm as a function of z . The flux limits chosen at each wavelength are expected to be reached by planned high galactic latitude imaging surveys with new space observatories in the next several years, as discussed above. The vertical axis is absolutely normalized to one steradian of sky coverage. In Table 1, we list the actual numbers of galaxies per steradian expected with redshifts above 1 and 2 in various flux-limited surveys. The next two columns give the total number and number with $z \geq 1$ for the fast evolution scenario.

The counts at a given observed flux level are dominated by the redshift at which L_* galaxies appear. As shown in Figure 3, the 120 μm *IRIS* and 25 μm *SIRTF* First Look surveys can both detect L_* galaxies up to $z \sim 0.6$. That is why the differential redshift distributions for all galaxies detected in these two surveys are predicted to be similar, as can be seen in Figure 7. For the baseline evolution scenario, we predict that 18% of the galaxies detected by *IRIS* will have $z > 1$, and 2% will have $z > 2$. For the fast evolution scenario, 24% of the detected galaxies will have $z > 1$ and 1% will have $z > 2$. *SOFIA* is expected to have comparable long-wavelength sensitivity to *IRIS* using 1 hour integrations with chopping (Becklin 1997).

Assuming that the *MIPS* “First Look” survey will cover five square degrees, our baseline model predicts integrated counts at 25 and 70 μm of 3900 and 6100 galaxies, respectively. Down to those flux limits, the cosmological depths are comparable, with median redshifts of 0.48 and 0.40, respectively, and upper quintile redshifts of 1.17 and 0.9. The baseline model predicts 25% and 5% of galaxies at 25 μm will have $z > 1$ and $z > 2$, respectively. The fast evolution model predicts these fractions are 33% and 3%. Reaching a factor of 3 deeper at 25 μm increases the depth to a median redshift of 0.8 and an upper quintile redshift of 1.64.

In a five square degree First Look Survey at 6 μm with *IRAC*, there should be a total of 9700 galaxies detected down to 30 μJy . Of these galaxies, 59% should have redshifts greater than 1, and 20 to 28% should have redshifts greater than 2. However, the reach would not be

greatly extended by much longer time integrations. Even at a limiting flux three times fainter ($10 \mu\text{Jy}$), the median redshift only increases from 1.30 to 1.44 and the upper quintile redshift increases from $z = 2.3$ to 2.46. This is because the First Look Survey with IRAC already reaches back to z_{flat} . Longer time integrations tend to detect more galaxies of lower luminosity with a similar redshift distribution.

The sensitivity of *FIRST* is also sufficient to detect the progenitors of modern L_* galaxies at all redshifts out to 5 (see Figure 3). At wavelengths longward of $100\mu\text{m}$, the sensitivity to high-redshift galaxies is comparable to that expected for IRAC at $6 \mu\text{m}$, owing to the positive K-corrections. We have approximated the imaging sensitivity of the Spectral and Photometric Imaging Receiver *SPIRE* on *FIRST* as 3.2 mJy at $250 \mu\text{m}$ (Griffin 1997), which might also be approached for small areas of sky by *SOFIA*. At this flux level, the strong positive K-correction results in a remarkably far reach for detection of distant galaxies: a median redshift of 1.62 and an upper quintile redshift of $z \geq 2.42$. A *PACS* survey to 5 mJy at $150\mu\text{m}$ (Poglitsch, 1997) will have a median redshift of 0.93 and an upper quintile of $z \geq 1.70$, with 47% of galaxies having $z > 1$ and 12% of galaxies having $z > 2$. It is gratifying to see that all of these planned surveys should detect high surface densities of galaxies at large redshifts.

The predicted confusion noise limits for the beamsizes of each of these instruments are also included in Table 1. These are very optimistically set to the flux levels at which there is an average of one source per beam. In reality, confusion becomes a problem when there is one source per 10 to 20 beams, so that the real confusion limits should probably be several times larger than the numbers quoted in the Table. The predictions are for the baseline evolution; the confusion limit fluxes are slightly larger in the fast evolution scenario. All of the planned surveys will be comfortably above the confusion limit except *SPIRE* $250\mu\text{m}$ imaging, which is close to the confusion-limit, and *IRIS* 120 and $150\mu\text{m}$ and *MIPS* $160\mu\text{m}$ imaging, which will be dominated by confusion noise.

9. Conclusions

We have used our empirically based model (MS98) to predict infrared luminosity functions and deep infrared galaxy counts at various wavelengths. We have also examined our predictions for the DIRB for comparison with the subsequent determinations from the *COBE-DIRBE* data analysis. Using the formalism of luminosity evolution proportional to $(1 + z)^Q$ out to a redshift of z_{flat} and constant (no further evolution) for $z_{flat} < z < z_{max} = 4$, we find that a comparison of their predictions with current *ISO* galaxy counts at 15 and $175\mu\text{m}$ favor our “Baseline Model” with $Q = 3.1$ and $z_{flat} = 2$ (the middle curve in Figure 2). The γ -ray limits (SD97) also favor $Q \sim 3$, as does a comparison of our predicted DIRB with the analysis of the *HEGRA* observations of high-energy γ -ray spectrum of Mrk 501 by Konopelko, Kirk, Stecker & Mastichidas (1999). On the other hand, the *COBE-DIRBE* far infrared determinations seem to favor a stronger evolution with $Q > 4$ up to $z_{flat} = 1$. For example, the upper curve in Figure 2 assumes $Q = 4.1$ and $z_{flat} = 1.3$.

This *prima facie* conflict can be resolved in two ways: either (a) the *COBE-DIRBE* far-infrared estimates may suffer from undersubtraction of foreground emission and therefore are too high, or (b) the *ISOPHOT* galaxy counts may be missing a significant fraction of sources. In this later case, one may also have to require that the γ -ray results are wrong in that the energies of photons detected by *HEGRA* have been overestimated, mimicing the effect which would be caused by absorption from a lower DIRB. Another possibility is one involving new physics, *viz.* that Lorentz invariance may be broken, allowing the Universe to be transparent to multi-TeV photons (Coleman & Glashow 1999; Kifune 1999; Glashow & Stecker 2000; Stecker 2000). This “new physics” scenario presents problems in that the Mrk 501 spectrum does exhibit exactly the characteristics expected for high-energy γ -ray absorption from pair-production (Konopelko *et al.* 1999).

Possibility (a) finds support in the independent analysis of the *COBE* data by Lagache *et al.* (1999) who obtain a flux at $140\mu\text{m}$ which is only 60% of the flux obtained by Hauser *et*

al. (1998) shown in Figure 1. Lagache *et al.* (2000) also obtained a smaller flux at 240 μm . In this regard, one should also note that the detections claimed by Hauser *et al.* (1998) were at the 4σ level.

If the far-infrared galaxy counts are incomplete (possibility (b)), this would imply stronger evolution in the far-infrared emission of galaxies than in the mid-infrared. Although the MS98 model already includes some differential evolution of this type, based on the data of Spinoglio *et al.* (1995), it is conceivable that starburst galaxies at redshifts ~ 1 might produce an even higher ratio of $\sim 60\mu\text{m}$ to $\sim 7\mu\text{m}$ rest-frame fluxes than their present-day counterparts. Radiation at these widely separated wavelengths is known to be emitted by quite different dust grains which could have a different evolutionary development, particularly for ULIRGs (ultraluminous infrared galaxies) and AGN (active galactic nuclei). One should note that this possibility can make the γ -ray and infrared data compatible, since absorption of ~ 15 TeV γ -rays is caused by interactions with mid-infrared ($\sim 20\mu\text{m}$) photons and not $140\mu\text{m}$ far-infrared photons.

We have shown here that planned infrared imaging surveys will soon be able to measure galaxy evolution out to redshifts of 2 or greater and help to resolve the question discussed above. This can be done with our simple modelling technique in conjunction with observations of luminosity functions, galaxy counts, and the diffuse infrared background.

A complete listing of the model count predictions at each wavelength can be obtained from the internet site www.astro.ucla.edu/faculty/malkan.html.

REFERENCES

Altieri, B. *et al.* 1999, A & A 343, L65

Becklin, E.E. 1997, Proceedings of ESA Symposium on “The Far-Infrared and Submillimeter Universe”, pg. 201

Biller, S.D. *et al.* 1998, Phys. Rev. Lett. 80, 2992

Blain, A.W. & Natarajan, P. 2000, MNRAS, 312, L39

Coleman, S. & Glashow, S.L. 1999, Phys. Rev. D59, 116008

Dole, H *et al.* 2000, astro-ph/0002283

Dwek, E. & Arendt, R. 1998, ApJ 508, L9

Elbaz, D. *et al.* 2000, A & A Letters, in press, e-print astro-ph/9910496

Fixsen, D.J. *et al.* 1998, ApJ 508, 123

Franceschini, A., *et al.* 1998, MNRAS 296, 709

Gispert, R, Lagache, G. and Puget, J. 2000, A & A, in press, e-print, astro-ph/0005554

Glashow, S.L. & Stecker, F.W. 2000, in preparation

Gorjian, V., Wright, E.L. & Chary, R.R. 2000, ApJ, 536, 550

Griffin, M. J. 1997, presentation at Grenoble meeting April 1997, <http://astro.estec.esa.nl/First>

Guiderdoni, B., Hivon, E., Bouchet, F. & Maffei, B. 1998, MNRAS 295, 877

Hauser, M., *et al.* 1998, ApJ 508, 25

Hopkins, A.M., Connelly, A.J. & Szalay, A.S. 2000, AJ, in press, e-print astro-ph/0009073

Juvela, M., Mattila, K. and Lemke, D. 2000, e-print, astro-ph/0005510

Kifune, T. 1999, ApJ 518, L21

Konopelko, A.K., Kirk, J.G. Stecker, F.W. & Mastichiadas, A. 1999, ApJ 518, L13

Lagache, G., Haffner, L.M., Reynolds, R.J. & Tufte, S.L. 2000, e-print astro-ph/9911355

Lawrence, A. *et al.* 1986, MNRAS 219, 687

Madau, P. Pozzetti, L. & Dickinson, M. 1998, ApJ 498, 106

Malkan, M.A., 1998 in *Astrophysics with Infrared Arrays: A Prelude to SIRTF*, Astron. Soc. Pacific, Conf. Series, in press, e-print astro-ph/9810055

Malkan, M.A., 2000, in *Our Second Look at the Immature Universe: The Infrared View*, Proc. Fourth RESCEU International Symposium, (Tokyo: Universal Academy Press) in press, e-print, astro-ph/0005251

Malkan, M.A. & Stecker, F.W. 1998, ApJ 496, 13 (MS98)

Poglitsch, A. 1997, presentation at Grenoble meeting April 1997, <http://astro.estec.esa.nl/First>

Pozzetti, L. *et al.* 2000, in *The Extragalactic Background and its Cosmological Implications*, IAU Symp. Vol. 204, ed. M. Harwit and M.G. Hauser, in press

Puget, J.L. *et al.* 1999, A & A 354, 29

Rush, B., Malkan, M.A. & Spinoglio, L. 1993, ApJS 89, 1

Saunders, W., *et al.* 1990, MNRAS 242, 318

Serjeant, S. *et al.* 2000, MNRAS, 316, 768

Shibai, H. 2000, Adv Space Res, 25, 2273

Soifer, B.T., *et al.* 1987, ApJ 320, 238

Spinoglio, L., *et al.* 1995, ApJ 453, 616

Spinoglio, L., *et al.* 2000, in preparation

Stanev, T. & Franceschini, A. 1998, ApJ 494, 159

Stecker, F.W., in *The Extragalactic Background and its Cosmological Implications*, IAU Symp. Vol. 204, ed. M. Harwit and M.G. Hauser, in press

Stecker, F.W. & De Jager, O.C. 1993, ApJ 415, L71

Stecker, F.W. & De Jager, O.C. 1997, in *Towards a Major Atmospheric Cerenkov Detector V*, Proc. Kruger National Park Workshop on TeV Gamma Ray Astrophysics, ed. O.C. De Jager (Potchefstroom: Wesprint) pg. 39

Steidel, C.C. *et al.* 1999, ApJ 519, 1

Takeuchi, T.T. *et al.* 1999, PASP 111, 288

Tan, C., Silk, J. and Balland, C. 2000, ApJ 522, 579

Totani, T. *et al.* in *The Extragalactic Background and its Cosmological Implications*, IAU Symp. Vol. 204, ed. M. Harwit and M.G. Hauser, in press

Xu, C. *et al.* 1998, ApJ 508, 576

Table 1: Predicted Galaxy Counts With Future Instruments

Instrument ($\lambda(\mu\text{m})$)	F_{lim}^a	N(Tot) ^b	N($z > 1$)	N($z > 2$)	Conf.Noise ^c
MIPS/SIRTF (25)	1.0	2.55(6)	6.3(5)	1.3(5)	3.2
” ”	”	4.57(6) ^d	1.5(5)	...	
MIPS/SIRTF (25)	0.32	1.34(7)	5.5(6)	1.5(6)	...
MIPS/SIRTF (70)	5.0	3.99(6)	6.7(5)	1.1(5)	130
IRAC/SIRTF (6)	.032	6.35(7)	3.8(7)	1.8(7)	0.1
” ”	”	8.86(7)	5.2(7)	...	
IRAC/SIRTF (6)	.01	2.37(8)	1.5(8)	7.7(7)	...
FIS/IRIS (120)	32	1.13(6)	2.1(5)	2.6(4)	21000
” ”	”	2.17(6)	7.5(5)	...	
FIS/IRIS (150)	50	7.38(5)	2.0(5)	3.0(4)	...
PACS/First (100)	5.0	9.94(6)	2.8(6)	4.8(5)	40
PACS/First (150)	5.0	2.16(7)	1.0(7)	2.5(6)	400
SPIRE/First (250)	3.2	5.45(7)	4.2(7)	1.8(7)	1100

- (a) Expected limiting fluxes are for 5σ -detections, in units of mJy.
- (b) Counts are given in scientific notation, with the exponent of 10 given in parentheses.
- (c) Confusion Limits, given in μJy , at which there is an average of one source per beam (FWHM).
- (d) The second line for each survey shows the galaxy number count predictions for the Fast Evolution scenario. At redshifts above $z = z_{flat} = 1.3$, there is no difference from the baseline model.

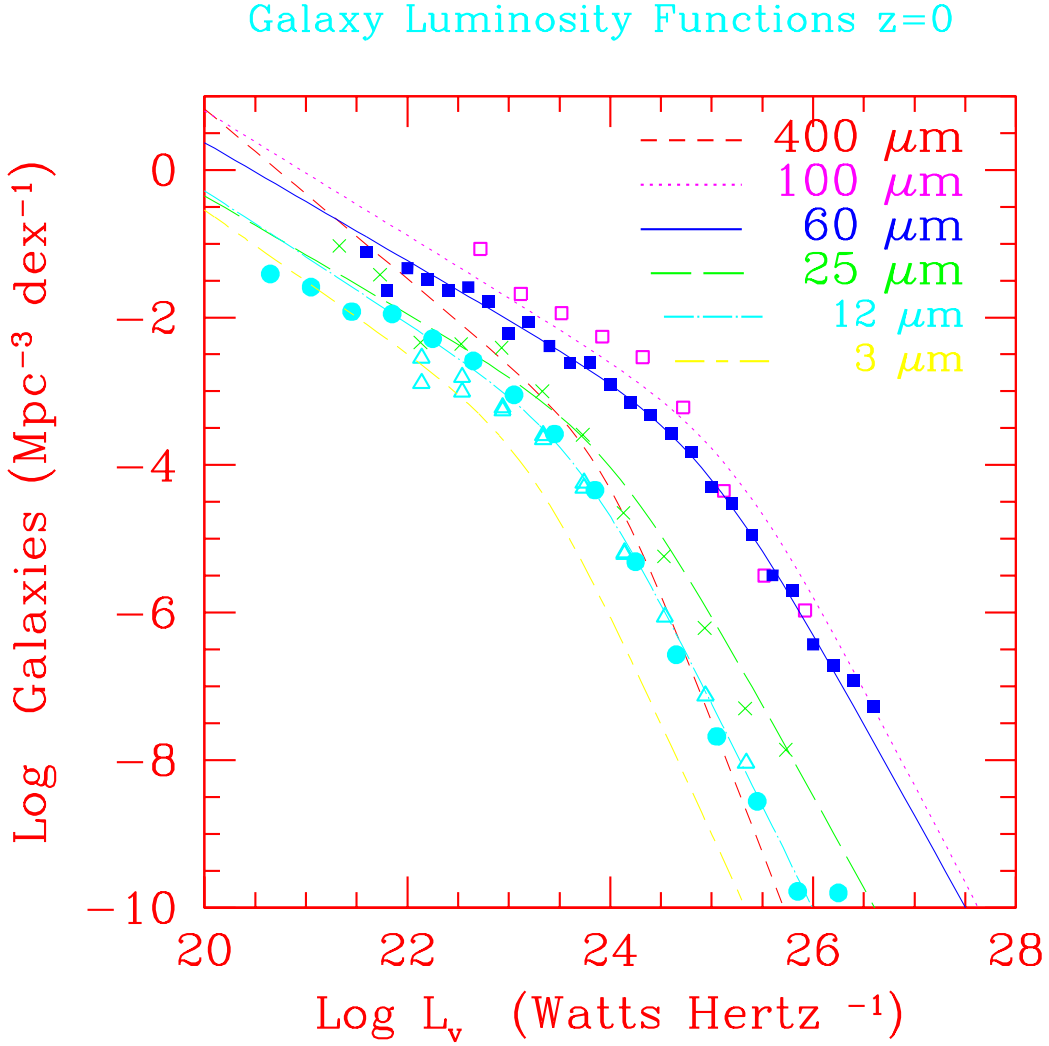


Fig. 1.— The family of infrared luminosity functions generated as described in the text. These are broken power-laws, where the characteristic turnover “knee” varies with wavelength. The solid squares show observations at $60\mu\text{m}$, which are well fitted by the model (long solid line). The open boxes are data from $100\mu\text{m}$, which fit the model dotted line. The X’s show data from $25\mu\text{m}$ for comparison with the long-dashed line model. And the solid circles and open triangles show observations of the $12\mu\text{m}$ luminosity function compared with the dot-dash line. Two other model LF’s are plotted for 3 and $400\mu\text{m}$, wavelengths at which there is no current observational comparison available.

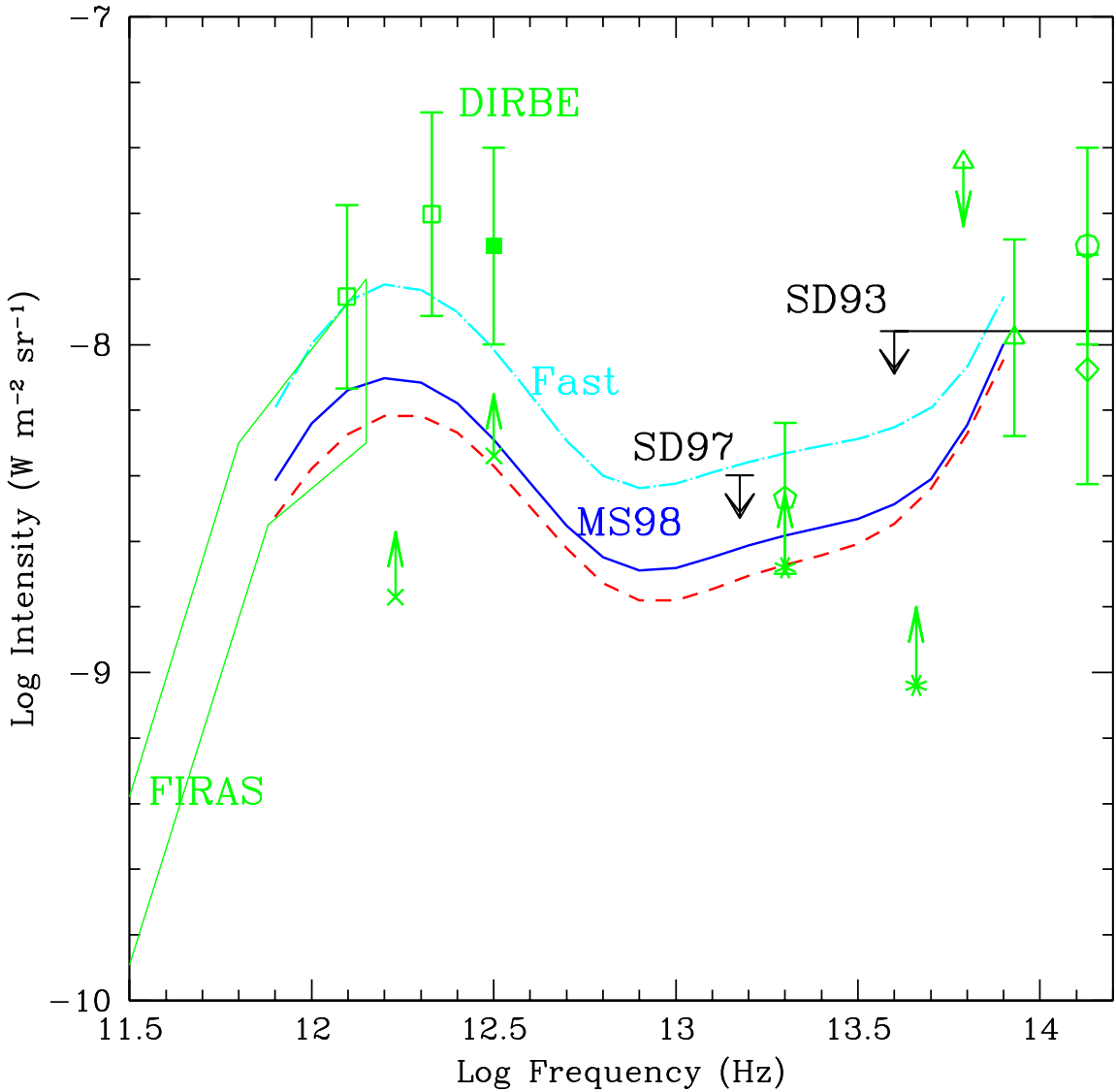


Fig. 2.— Spectral energy distributions (SEDs) of the diffuse infrared background (DIRB) calculated using the models described in the text and compared with representative data given with 2σ error bars. The FIRAS range is illustrated with a polygon. From left to right, open squares: Hauser *et al.* (1998), solid square: Lagache (2000), pentagon: Altieri *et al.* (1999), open triangles: Dwek and Arendt (1998), open circle: Gorjian, Wright & Chary (2000), diamond: Totani, *et al.* (2000) (see also Pozzetti *et al.* (2000)). The lower limits with crosses are based on integrals of deep source counts from *ISOPHOT* (Puget *et al.* 1999) and the lower limits with asterisks are from *ISOCAM* (Elbaz *et al.* (1999)). The upper limits are from Stecker & de Jager (1993)(SD93) and Stecker & de Jager (1997)(SD97).

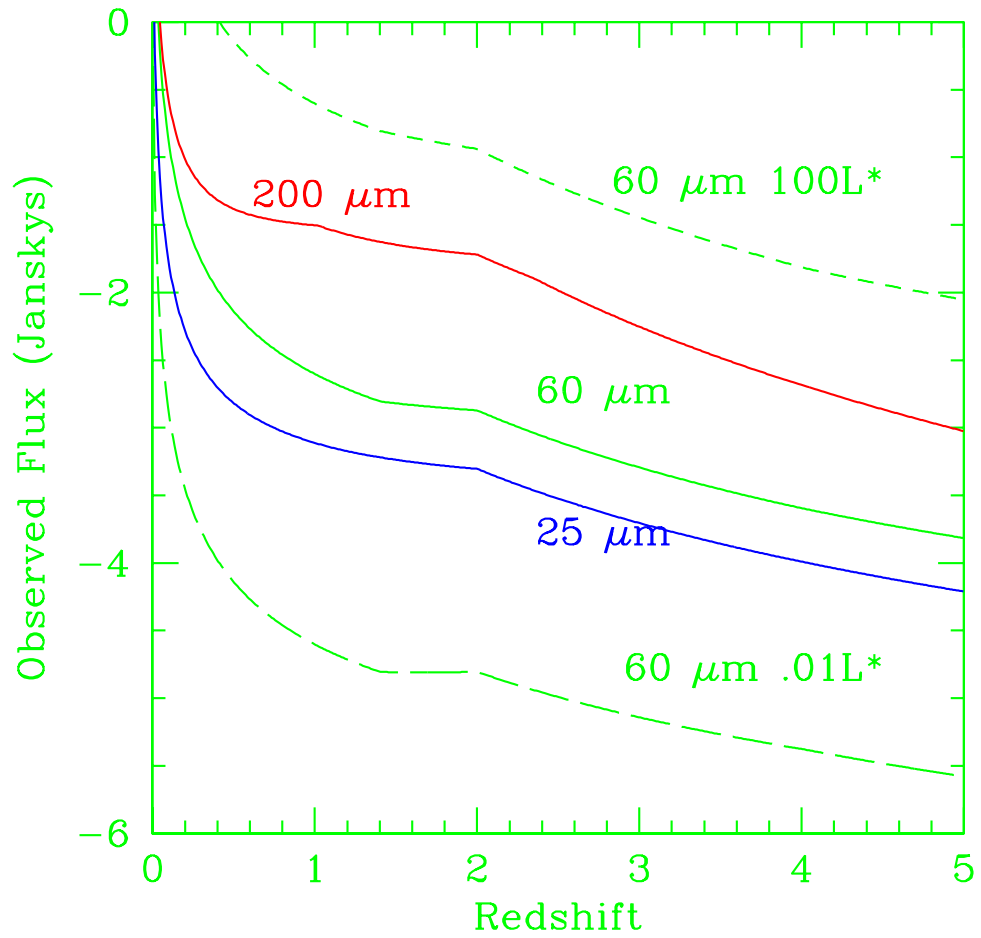


Fig. 3.— The observed flux as a function of redshift for galaxies with L_* at $z = 0$ at 25, 60 and 200 μm , and at 60 μm for galaxies of luminosities 0.01 L_* and 100 L_* (dashed lines). These estimates are for the baseline evolution of $Q = 3.1$ up to $z_{flat} = 2$.

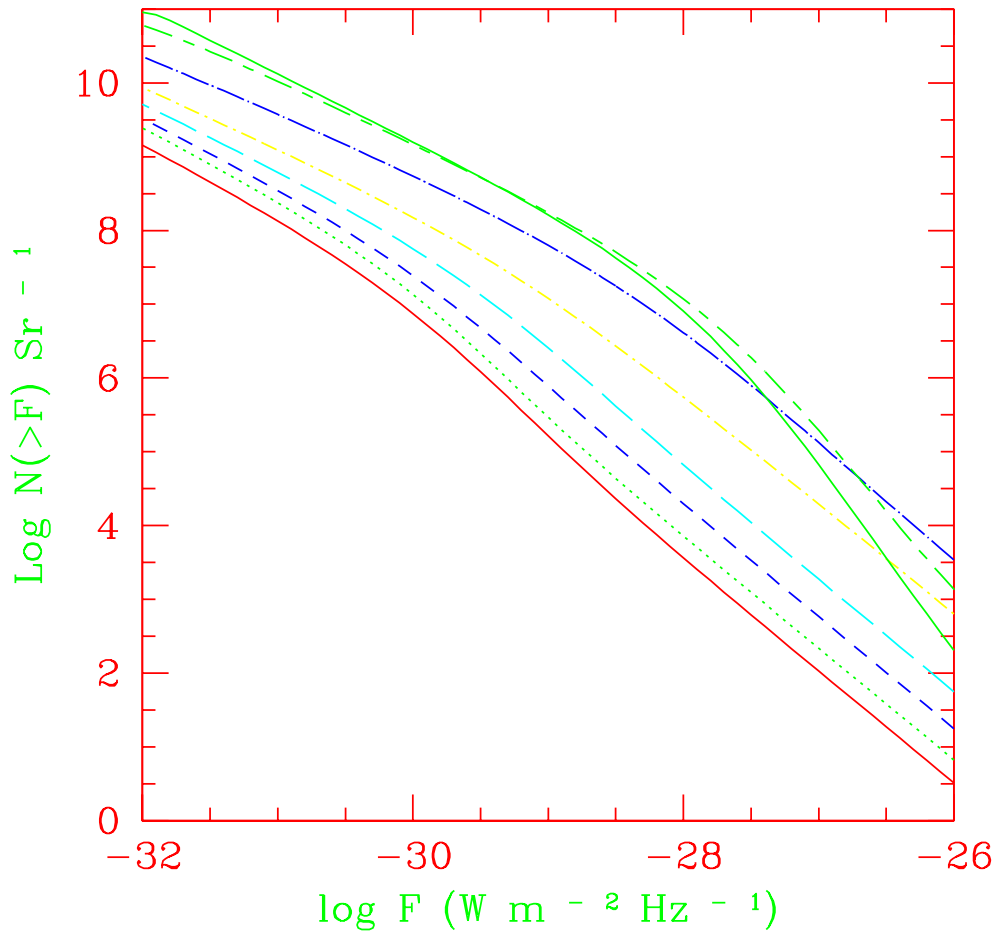


Fig. 4.— Galaxy count predictions for the baseline model at eight representative wavelengths. Solid lines are at 3 and $400\mu\text{m}$ (bottom and top). The dotted line is for observations at $6\mu\text{m}$; short dashes $12\mu\text{m}$; long dashes $25\mu\text{m}$, dot-dash $50\mu\text{m}$, dot-long dash $100\mu\text{m}$, and long dash-short dash $200\mu\text{m}$. Except at the longest wavelengths, most of the models show the expected Euclidean slope of $-3/2$ at the bright end. All models turn flatter than this at the faintest fluxes due to cosmological factors.

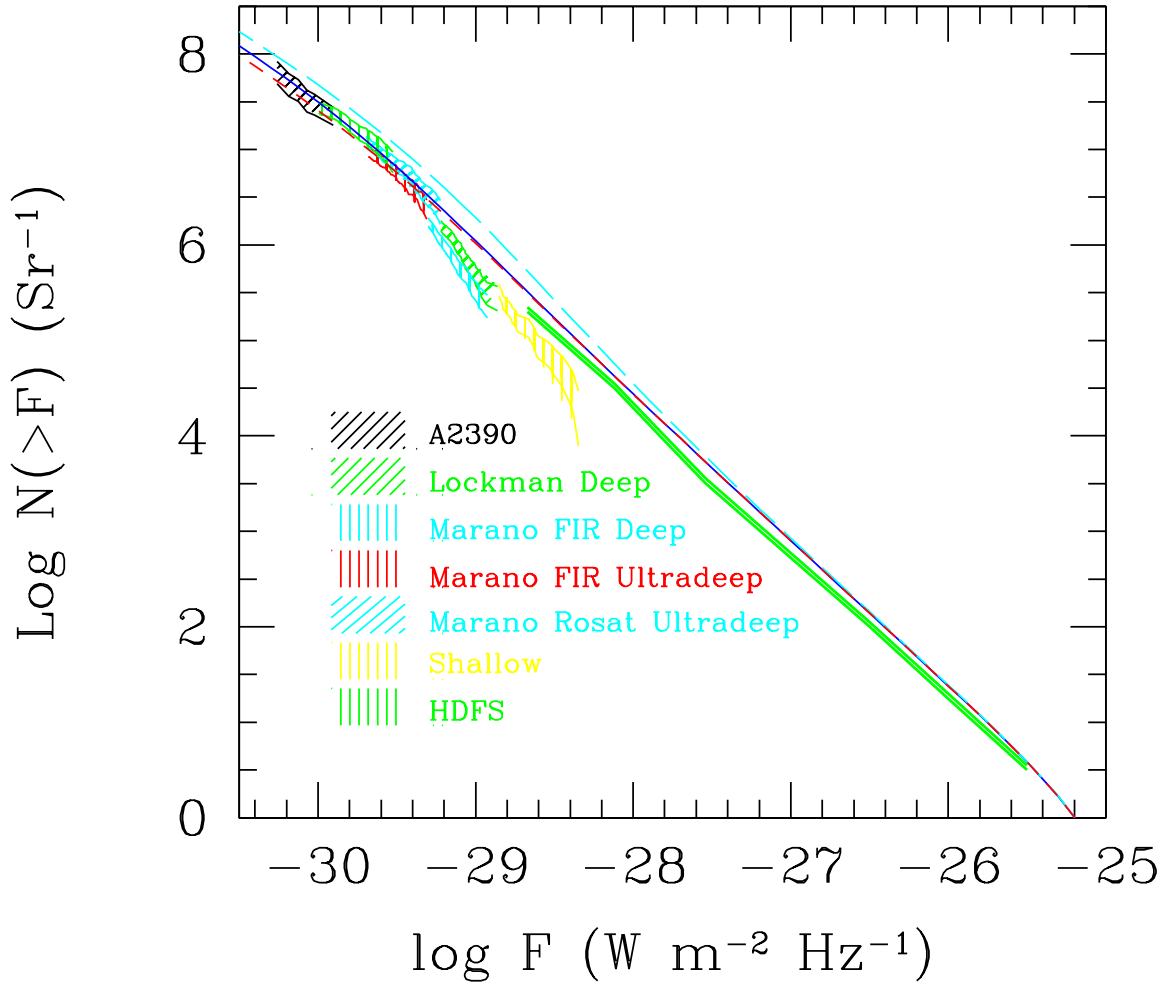


Fig. 5.— Galaxy counts predicted for our various evolution models at $15 \mu\text{m}$ compared with the data compiled by Elbaz *et al.* (2000), and from Sejeant *et al.* (2000: thick line). Error ranges of 1σ are shown. The solid line shows the baseline model; the dashed line is the lower limit ($z_{flat} = 1$), while the dot-dash line shows the fast evolution model ($Q = 4.1$ up to $z_{flat} = 1.3$).

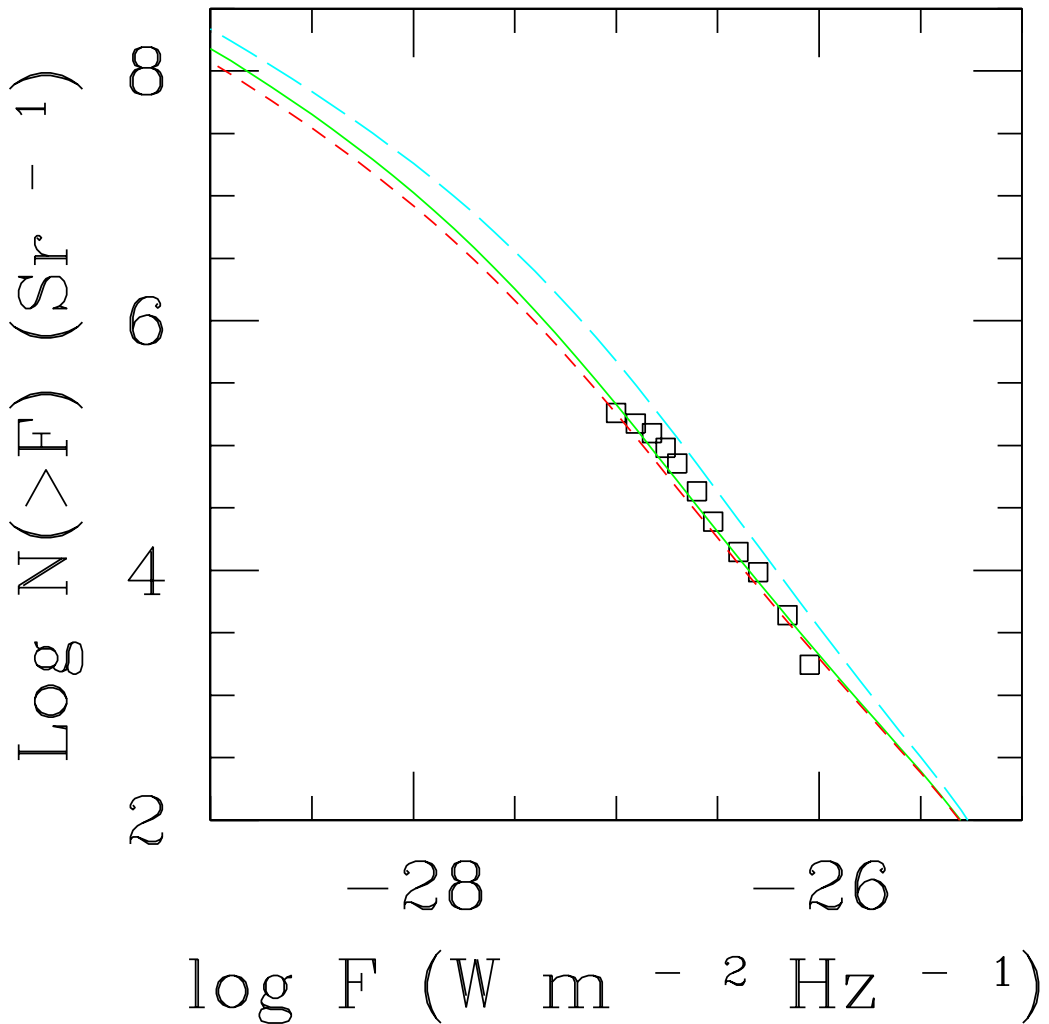


Fig. 6.— Galaxy counts at 175 μm predicted for our various evolution models compared with the data (open squares) compiled by Puget *et al.* (1999). Models are illustrated with the same line styles as in Figure 5.

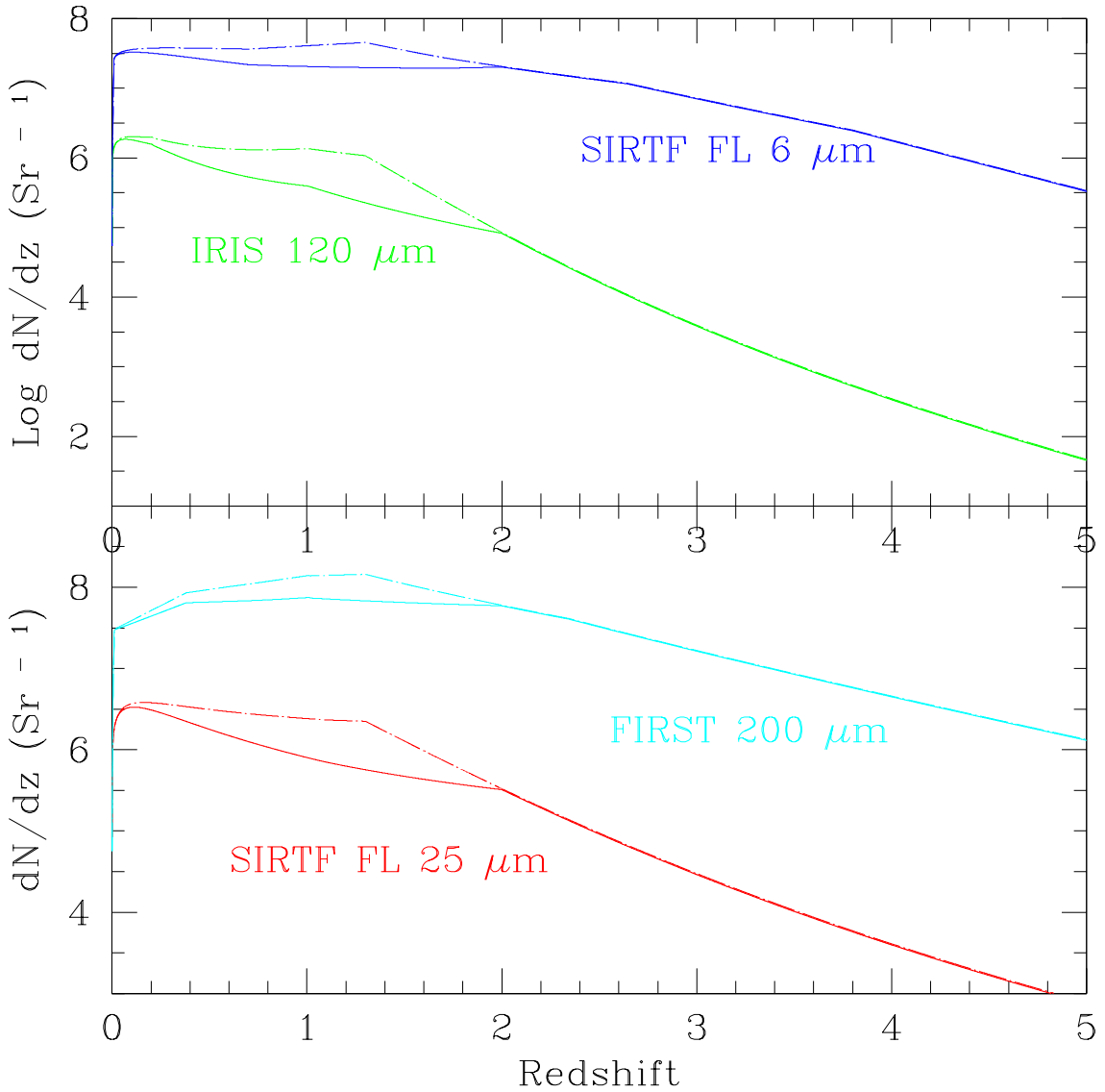


Fig. 7.— Number of observable sources in flux-limited samples covering one Steradian of sky, as a function of redshift for planned space infrared telescopes as described in the text. The solid lines are for the baseline model. The dot-dash line are for the fast evolution case, which has the greatest excess of galaxies at its value of $z = z_{flat} = 1.3$. Note that the *SIRTF* First Look Survey at $6\mu\text{m}$ and *FIRST* survey at $200\mu\text{m}$ have comparable depths, as do the *IRIS* and *SIRTF/MIPS* surveys.